Solid Freeform Fabrication 2023: Proceedings of the 34th Annual International Solid Freeform Fabrication Symposium – An Additive Manufacturing Conference
Reviewed Paper

EXPLORATORY STUDY OF IN-SPACE WIRE ARC ADDITIVE MANUFACTURING WITH MODELING APPROACH

Wei Li*, Dan Bouzolin*, and Kishore Mysore Nagaraja*

*Department of Mechanical Engineering, The University of Texas at Dallas, Richardson, TX 75030

Abstract

Countries all over the world are rushing into space exploration due to crisis of energy and resources exhaustion on the Earth. Mars is an obvious target because it has a thin atmosphere, good geological similarity, and is close by in the Solar system. As the satellite of the Earth, Moon is another target since it is very close to the Earth. For the large spacecrafts such as Mars rovers, periodic maintenance is necessary to ensure the completion of long-duration exploration missions. In-space wire arc additive manufacturing (WAAM) provides a potential solution towards sustainable maintenance with onsite repair or additive manufacturing. For in-space manufacturing, reduced gravity is an important factor. In this work, WAAM processes under reduced gravity conditions on the Mars and Moon were studied through a multi-physics modeling approach. The metal droplet transfer, deposition geometry, thermal dissipation, and other key physics in WAAM were simulated. To validate the modeling approach, an experimental case was conducted on an in-house WAAM platform under the Earth condition.

Keywords: Wire arc additive manufacturing, thermal-fluid model, In-space manufacturing, reduced gravity, space exploration.

Introduction

In-Space Manufacturing (ISM) provides a solution toward establishing a sustainable human presence on Mars, the Moon, or space stations, through on-site additive manufacturing technologies (Fig 1). For ISM, reduced gravity is an important consideration in the manufacturing process. In this work, a Wire-Arc Additive Manufacturing (WAAM) technique was explored and validated against Earth gravity. A multi-physics model was used to simulate the WAAM process. The model was then subsequently applied to low-gravity environments such as on Mars and the Moon. This work is an exploratory study for space exploration plans in the future.

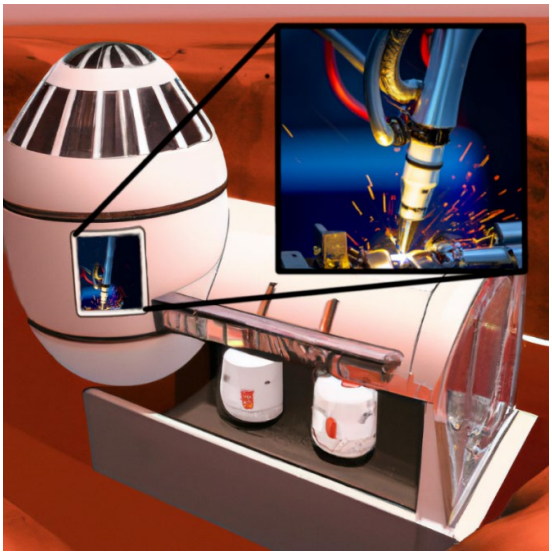

Fig 1 In-space manufacturing concept, with a close-up of an example welding process

Wire-Arc Additive Manufacturing (WAAM) is an advanced fabrication technique that uses an electrical arc to melt a metal wire for layer-by-layer deposition [1-5], as shown in Fig 2. WAAM can be used to create near

net shape part geometries, making it highly desirable for material savings relative to subtractive processes like machining [6-8]. WAAM can also be used for repairing existing components as an alternative to traditional processes such as MIG and TIG welding [6, 9-11]. The WAAM process provides a high deposition rate, allowing it to produce parts quickly. The flexibility of WAAM in part geometry and rapid prototyping means that tangible cost and time savings can be achieved using this process[2, 9, 12-15].

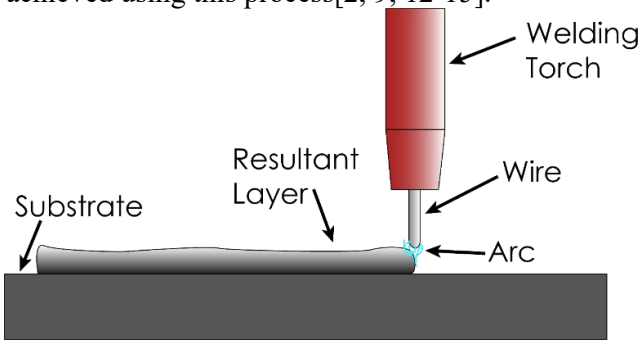

Fig 2 Overview of the wire-arc additive manufacturing process setup

To study the WAAM process under the reduced gravity conditions, modeling approach is a needed since it is challenge to conduct the WAAM experiment under the required reduced gravity environment. The WAAM process is normally difficult to model due to the complexity of the physical interactions involved, which include effects of electromagnetism, the Joule effect and radiation of the plasma[13, 14]. This research work aims to mitigate this fact by leaving out these complex electromagnetic effects and electrical arc modeling, instead approximating the heat source as a pulsed heat source with Gaussian energy distribution. The benefit of this approach is that the overall simulation is less computationally expensive, allowing for rapid modeling and testing as well as larger part geometries.

Methods, Models, and Experiment

The model for this experiment consists of two major components: the metal wire (being fed from the robotic welding arm) and the substrate (onto which the metal wire is deposited). The wire and substrate material used for WAAM deposition is mentioned in Table 1. Both parts were modeled directly in Flow3D [16] as aluminum components. The model uses an electric heat source to simulate the heat input from the electrical arc of the welding machine. The fundamentals of the thermal-fluid, electric heat source, heat transfer, phase change, and other multiple physics were referred from the publication [14]. The Fig 3 as below shows the final part modeled in Flow3D with geometric parameters taken from the physical model. The part geometry was modeled as a solid block of aluminum substrate (shown in blue) with a phantom region (shown in red) used to control the feed rate of the wire. The part was meshed in three regions: one center region (shown by the green lines) which has a cell size of 3e-4 m, and two side regions (shown by the cyan lines) which use a cell size of 5e-4 m. The higher fidelity in the center allows for more accurate modeling of surface tension while the coarser mesh on the outside keeps the simulation runtime down. Upon meshing, running, and rendering the results, the simulation setup functions as the experiment does with the wire feed, heating, and traversal.

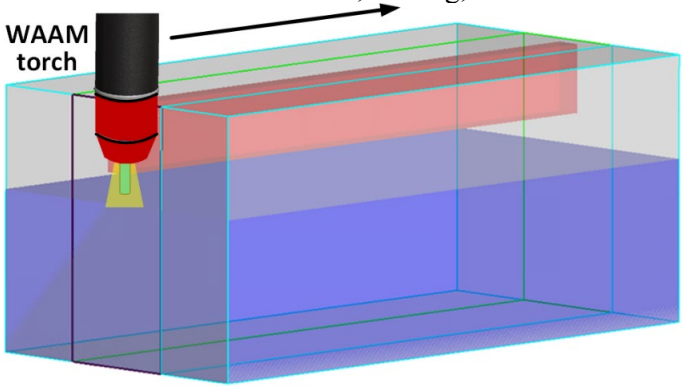

Fig 3 Flow3D model of final part geometry and mesh block delineations

The physical parts were printed using the ABB IRB 140 robotic arm and Fronius TPS 320i electric welding system, as shown in Fig 4. A wire diameter of 1 mm was used for the printing process. The wire feed rate is approximately 250 mm/s and the surface traversal rate is 30 mm/s. The power input into the system was calculated as 2154 W, which was obtained from the specifications used in the Fronius machine (136 A * 19.8 V * 80% = 2154 W) with 80% as the power efficiency. This power input was then pulsed at 20 Hz by using a transient power input file to mimic the behavior of the experimental setup. The substrate dimensions are 50 x 25 x 13 mm, with the wire traversal direction along the longest dimension of the substrate.

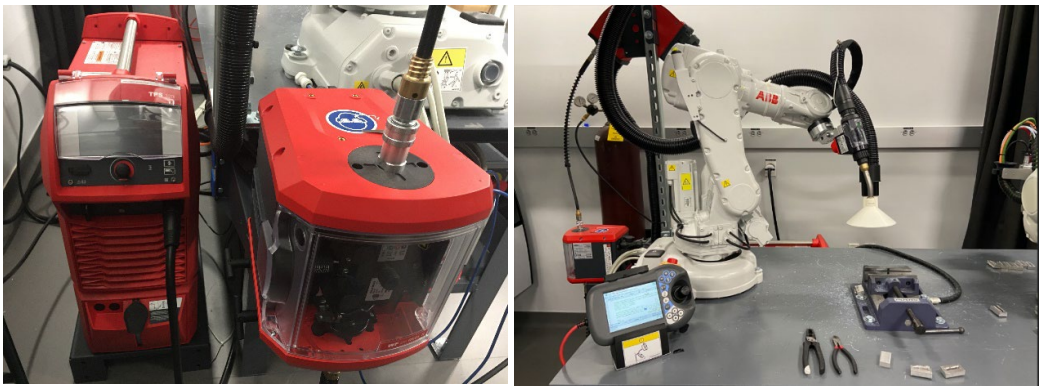

Fig 4 Fronius welding system (left) and ABB robotic welding arm (right) used in the experiment

The experimental part dimensions and welding setup parameters were input into the Flow3D software to run the simulation. The simulation was an iterative process, with parameters needed to be tuned in order to match the simulated model, but the final parameters lent themselves to relatively close correlation in simulated and experimental results. The material data of temperature-dependent properties of the Al 6061 alloy was used in the model. The simulation was run with Al 6061 wire, which has readily available data on how density, dynamic viscosity, thermal conductivity, and specific heat of the material all vary with temperature increase.

Table 1 Summary table of parameters used in the simulation

Substrate Material	Al 6061
Wire Material	Al 6061
Wire Feed Rate	250 mm/s
Wire Traversal Speed	30 mm/s
Power Input	2693 W @ 20 Hz
Substrate Length	50 mm
Substrate Width	25 mm
Substrate Height	13 mm
Shield Gas Velocity	50 m/s
Shield Gas Density	1.225 kg/m^3

The final parameters are listed in Table 1 as above, but several parameters had to be tuned in order to more closely match the experimental results. For example, the wire feed rate and wire traversal speed have a significant effect on the overall behavior of the wire as it feeds down toward the substrate, as well as the physical material deposition process. With these parameters set too fast, the wire has no time to form droplets of molten metal, and instead feeds solid material directly onto the substrate. With the parameters set too slow, the metal droplet accumulates too much volume as it continues to be heated by the power source, and therefore does not continuously deposit, only depositing once the volume grows too large. Finally, the shield gas flowrate provides a downward force that pushes the droplet towards the substrate. With this parameter set too low, the droplet does not deposit onto the substrate, instead bubbling up on itself due to the force of the surface tension within the droplet.

Results and Discussion

The results of the Earth gravity simulation were first validated against experimental part geometry. The experiment takes 1.7 seconds to deposit one layer of metal onto the substrate. The simulation also models 1.7 seconds of WAAM process, but takes about 20 hours to run. The main parameter of interest between the experiment and simulation is the overall layer geometry, which includes the layer width and height along the length of the substrate. The Fig 5 illustrates the experimental and simulated part geometries after undergoing the WAAM process.

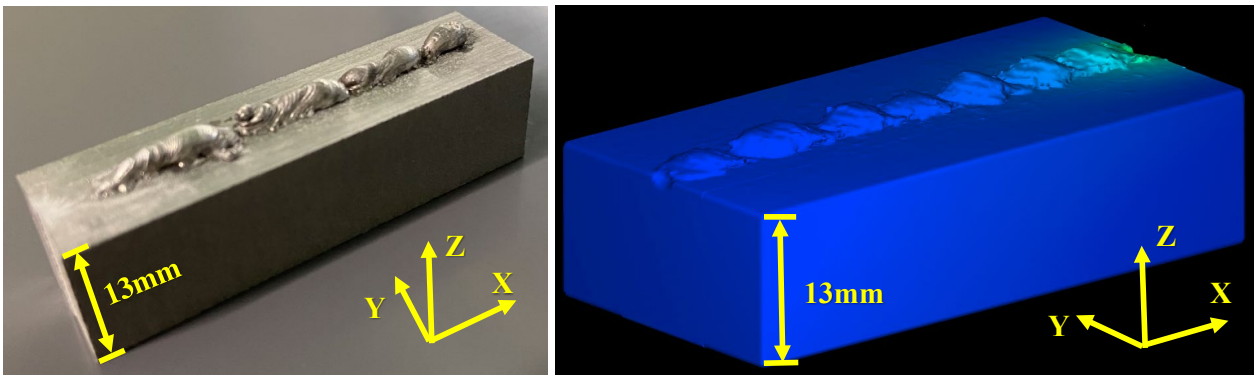

Fig 5 Experimental part geometry (left) vs simulated part geometry (right) using WAAM process

The experimental part geometry and simulated part geometry are in relatively close agreement, with a few minor differences. First, the experimental part geometry shown has an overall smaller bead width than the simulated part geometry, giving the appearance of a much larger aspect ratio in terms of the layer height. In fact, the regions printed with the WAAM process are similar in size between both the simulation and experiment. The Fig 6 as below shows a side view with a more comparable look at the printed part geometries.

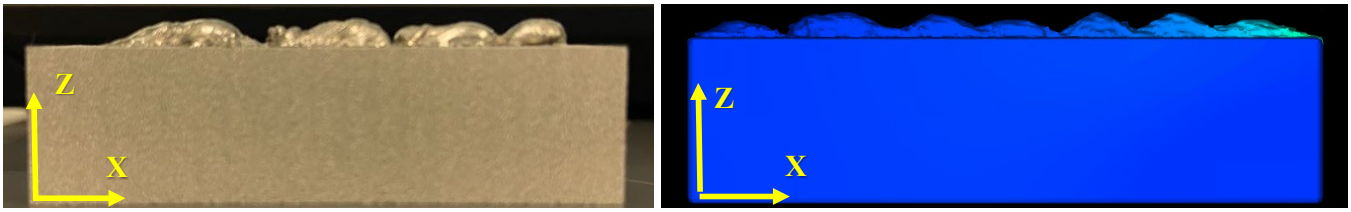

Fig 6 Side views comparison of experimental part geometry (left) vs simulated part geometry (right)

In addition, the front view of the part geometries is shown in Fig 7 as below, illustrating the width of the printed features resulting from the WAAM process.

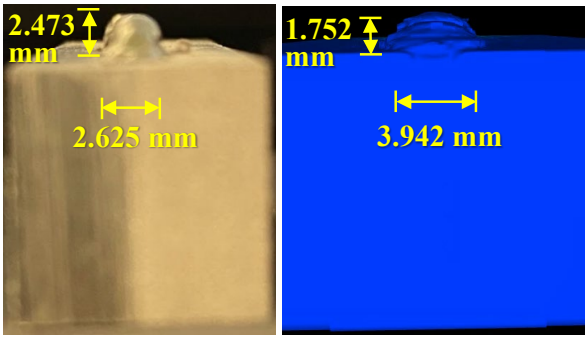

Fig 7 Front view comparison of experimental part geometry (left) vs simulated part geometry (right)

From an initial inspection, the experimental part geometry appears slightly taller while the simulated part geometry appears slightly wider. To quantify these relative differences between the simulated and experimental

parts, the sizes of the printed features were measured. Table 2 below shows the quantitative difference in printed part geometry between the experimental and simulated parts.

Table 2 Summary table of printed part geometry

Sample Type	Maximum Print Height (mm)	Maximum Print Width (mm)
Experimental	2.42	3.70
Simulated	2.09	4.78

To understand these differences, it is important to understand how the WAAM process works: more specifically, how material is deposited onto the substrate. The primary mechanism by which metal is melted and deposited onto the substrate is through a droplet-based deposition process. The heat source melts the incoming wire, which bubbles up into a droplet with nearby liquid metal. Once the droplet is big enough, it detaches from the wire and deposits onto the substrate below.

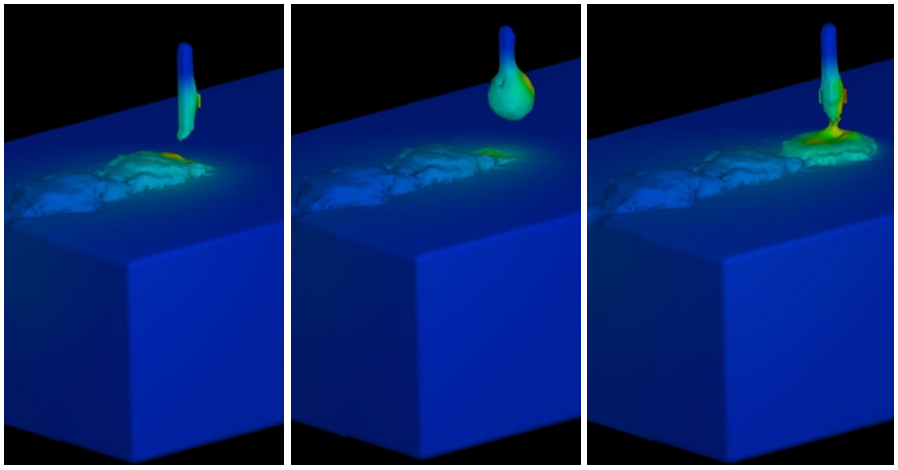

(a) (b) (c)

Fig 8 Droplet-based deposition process with (a) initial wire, (b) material accumulation, and (c) droplet deposition

As mentioned before, the experimental part geometry had slightly taller ridges while the simulated part geometry had slightly wider ridges. The reason for this difference becomes apparent upon closer inspection of Fig 8, which depicts the droplet-based deposition process. Though this minor difference exists between the experiment and simulation, the overall modeling of the WAAM process and droplet deposition were sufficient to continue with further simulation. Once the results of the Earth-gravity simulation were validated against the experimental part geometry, a baseline was established for which to compare future simulations to. To simulate the physics of acceleration due to gravity, the z-component of gravity in the simulation was set to the various values ranging from Earth gravity (-9.81 m/s^2) to Moon gravity (-1.62 m/s^2). A summary of the parameters that were updated for this investigation is shown in Table 3 below.

Table 3 Summary table of gravity parameters used for different simulations

Simulation Number	Simulated Environment	Acceleration due to Gravity (m/s^2)
1	Earth	-9.81
2	Moon	-1.62
3	Mars	-3.72

Upon changing the gravity, the simulation was re-run for each scenario. The results for both the Mars gravity simulation and Moon gravity simulation are summarized in the Fig 9 as below.

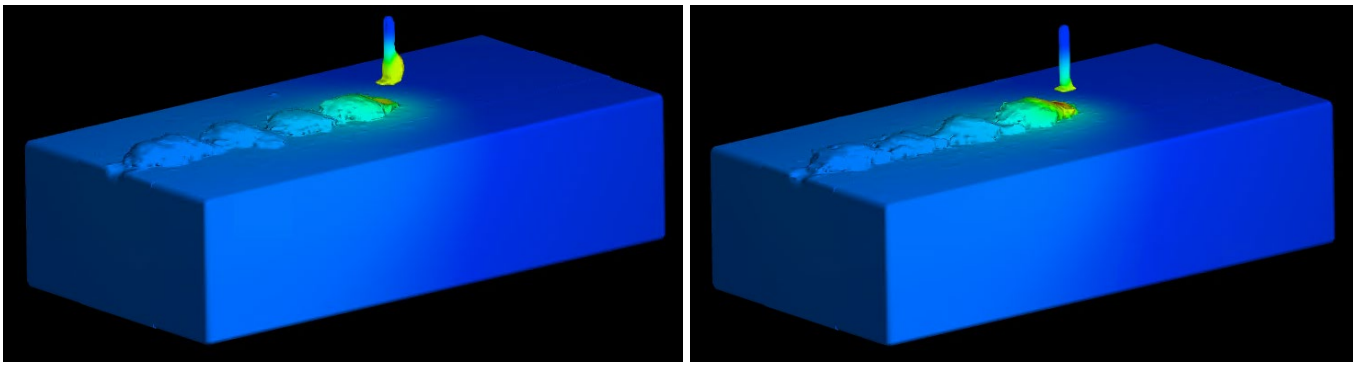

Fig 9 Comparison of Mars gravity simulated result (left) and Moon gravity simulated result (right)

Upon inspection, the two results show close correlation with each other as well as with the Earth gravity result. The overall part geometry remains similar between trials, indicating that the change in gravity may not be the driving factor in droplet deposition. From the droplet-based deposition process in Fig 8, the droplet deposits onto the substrate upon growing large enough to touch the surface, at which point the contact force from touching the substrate overcomes the surface tension within the droplet keeping it together. Because the droplet does not break off prior to touching the surface, the force of gravity does not have as significant of an effect as other forces such as the wire feed rate and downward force due to the shield gas.

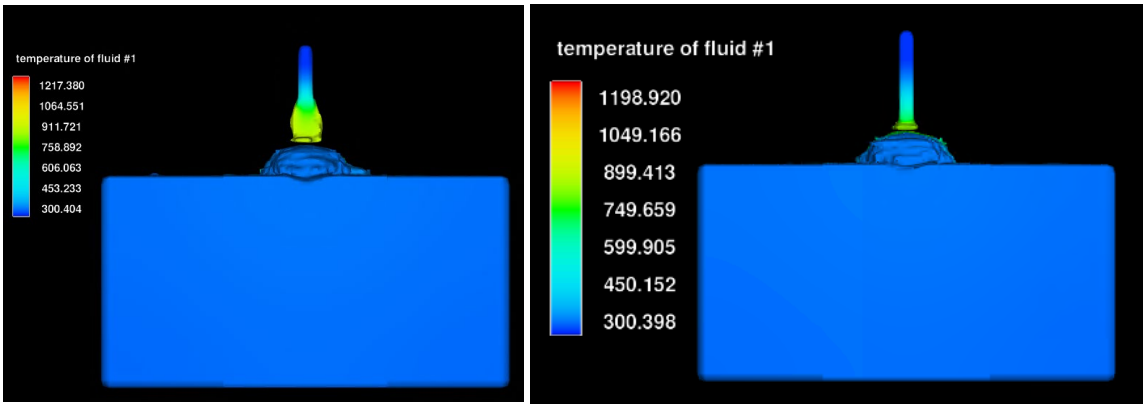

Fig 10 Front view of Mars simulation result (left) and Moon simulation result (right)

The front views of each simulation (Fig 10) show close correlation to one another as well as the Earth gravity result. Though the gravity varies from Earth gravity by nearly 3x for the Mars simulation and 6x for the Moon simulation, the overall part width remains consistent. The heights of the resultant printed features remain consistent between simulations, which can be validated further using the side views of each part.

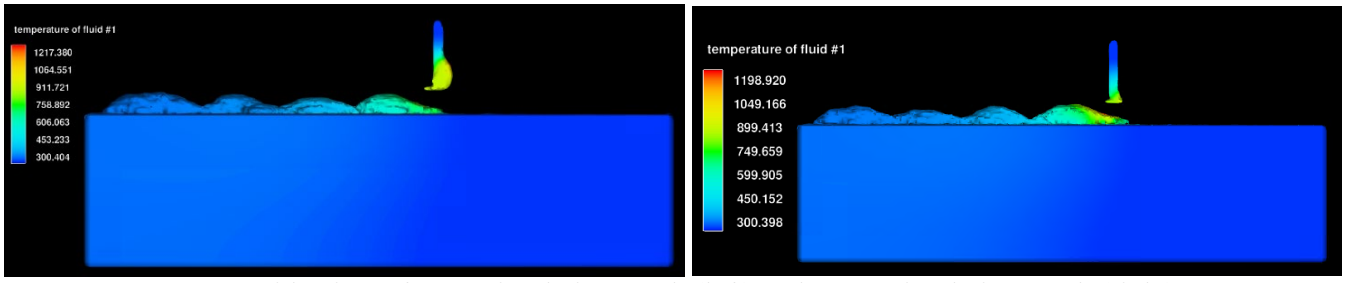

Fig 11 Side view of Mars simulation result (left) and Moon simulation result (right)

From the side views of both low-gravity simulations (Fig 11), it becomes clear that the droplet formation process develops features with similar heights, with only slight variation between each ridge as to where the height grows smaller or larger. The side view also provides valuable insight into the location at which droplets

are formed. If gravity were to add a substantial force pulling down the droplets toward the substrate, it would be expected to see droplets forming smaller ridges but more frequently along the substrate. However, the droplets form in the same locations each time, giving rise to consistently manufactured ridges between each case. We can further inspect the top view to validate the droplet formation locations along the substrate.

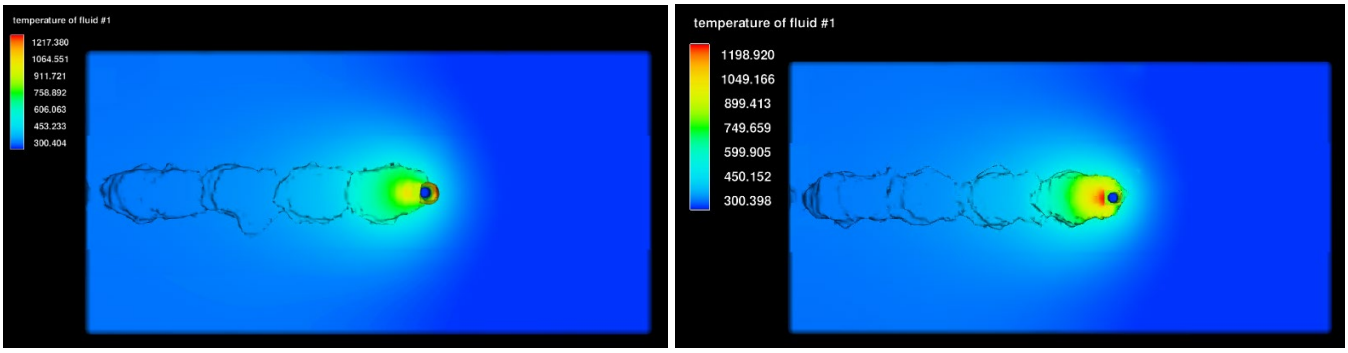

Fig 12 Top view of Mars simulation result (left) and Moon simulation result (right)

Comparing the top views of both low-gravity simulations (Fig 12), it shows that the droplets formed during the WAAM process detach at approximately the same locations and at the same time in both simulations. The results indicate that the WAAM process has no issue with droplet formation in such low-gravity environments, owing to the fact of several forces acting in tandem on the droplet in addition to gravitational force.

Conclusion

The results of the Earth gravity simulation were first validated against experimental part geometry. The electric heat source was effective at heating the wire for melting, as evidenced by the general wire melt pattern matching between the experimental and simulated results. However, improvements could be made to approximate the wire-arc behavior, as the pulsed electric heat source does not transfer as much heat to the substrate in the simulation compared to the wire arc in the experiment.

As evidenced from the figures above, varying the acceleration due to gravity did not have a significant effect on the simulation results. This suggests that the droplet-based deposition process may not be driven strictly due to gravity, but may be driven by other, more significant factors, such as the wire feed rate and the force on the fluid due to the incoming shield gas.

The simulated results show that the wire-arc additive manufacturing process may be extended to in-space manufacturing with few differences from what is seen currently on Earth. However, caution should be exercised in extending this result, as the simulation and experiment only correlated the first layer of the WAAM process. More work can be done to identify how the parts vary with multiple printed layers.

In general, this study provides an overview of the wire-arc additive manufacturing process and the effects of varying gravity on this process. Preliminary work shows that the wire-arc additive manufacturing process is suitable for in-space manufacturing, with only minor differences in part geometry between parts printed in Earth gravity versus Mars or Moon gravity. Future studies can explore changing the heat source to approximate the wire-arc more closely in the simulation as well as printing multiple layers at a time, both of which would provide valuable information about the validity of WAAM for in-space manufacturing.

Reference

[1] C. Cunningham, J. Flynn, A. Shokrani, V. Dhokia, S. Newman, Invited review article: Strategies and processes for high quality wire arc additive manufacturing, Additive Manufacturing 22 (2018) 672-686.
[2] S.K. Dash, Study of Wire Arc Additive Manufacturing With Aluminum Alloy 2219, (2019).
[3] Y. Ali, P. Henckell, J. Hildebrand, J. Reimann, J. Bergmann, S. Barnikol-Oettler, Wire arc additive manufacturing of hot work tool steel with CMT process, Journal of Materials Processing Technology 269 (2019) 109-116.
[4] A. Balanovskiy, N. Astafyeva, V. Kondratyev, A. Karlina, Study of mechanical properties of C-Mn-Si composition metal after wire-arc additive manufacturing (WAAM), CIS Iron and Steel Review 22 (2021) 66-71.
[5] J. Sun, J. Hensel, M. Köhler, K. Dilger, Residual stress in wire and arc additively manufactured aluminum components, Journal of Manufacturing Processes 65 (2021) 97-111.
[6] J.-H. Lee, C.-M. Lee, D.-H. Kim, Repair of damaged parts using wire arc additive manufacturing in machine tools, Journal of Materials Research and Technology 16 (2022) 13-24.
[7] F. Michel, H. Lockett, J. Ding, F. Martina, G. Marinelli, S. Williams, A modular path planning solution for Wire+ Arc Additive Manufacturing, Robotics and Computer-Integrated Manufacturing 60 (2019) 1-11.
[8] R. Wang, H. Zhang, W. Gui-Lan, X. Zhao, Cylindrical slicing and path planning of propeller in wire and arc additive manufacturing, Rapid Prototyping Journal (2020).
[9] C. Xue, Y. Zhang, P. Mao, C. Liu, Y. Guo, F. Qian, C. Zhang, K. Liu, M. Zhang, S. Tang, Improving mechanical properties of wire arc additively manufactured AA2196 Al–Li alloy by controlling solidification defects, Additive Manufacturing 43 (2021) 102019.
[10] B. Wu, Z. Pan, D. Ding, D. Cuiuri, H. Li, J. Xu, J. Norrish, A review of the wire arc additive manufacturing of metals: properties, defects and quality improvement, Journal of Manufacturing Processes 35 (2018) 127-139.
[11] C. Zhang, Y. Li, M. Gao, X. Zeng, Wire arc additive manufacturing of Al-6Mg alloy using variable polarity cold metal transfer arc as power source, Materials Science and Engineering: A 711 (2018) 415-423.
[12] A.R. McAndrew, M.A. Rosales, P.A. Colegrove, J.R. Hönnige, A. Ho, R. Fayolle, K. Eyitayo, I. Stan, P. Sukrongpang, A. Crochemore, Interpass rolling of Ti-6Al-4V wire+ arc additively manufactured features for microstructural refinement, Additive Manufacturing 21 (2018) 340-349.
[13] D. Ding, Z. Pan, D. Cuiuri, H. Li, A multi-bead overlapping model for robotic wire and arc additive manufacturing (WAAM), Robotics and Computer-Integrated Manufacturing 31 (2015) 101-110.
[14] S. Cadiou, M. Courtois, M. Carin, W. Berckmans, 3D heat transfer, fluid flow and electromagnetic model for cold metal transfer wire arc additive manufacturing (Cmt-Waam), Additive Manufacturing 36 (2020) 101541.
[15] D. Ding, Z. Pan, D. Cuiuri, H. Li, S. van Duin, N. Larkin, Bead modelling and implementation of adaptive MAT path in wire and arc additive manufacturing, Robotics and Computer-Integrated Manufacturing 39 (2016) 32-42.
[16] W. Li, M. Kishore, R. Zhang, N. Bian, H. Lu, Y. Li, D. Qian, X. Zhang, Comprehensive studies of SS316L/IN718 functionally gradient material fabricated with directed energy deposition: Multi-physics & multi-materials modelling and experimental validation, Additive Manufacturing 61 (2023) 103358.